Theor Chem Acc (2012) 131:1133
DOI 10.1007/s00214-012-1133-y

REGULAR ARTICLE

Thermodynamic and stereochemical aspects of the polymerizability of glycolide and lactide

Carlos Alemán · Oscar Bertran · K. N. Houk · Anne Buyle Padías · Henry K. Hall Jr.

Received: 15 June 2011 / Accepted: 25 August 2011 / Published online: 16 February 2012

Abstract The ring-opening polymerizations of the dilactones glycolide and the *S*,*S*- and *S*,*R*-stereoisomers of lactide were studied using quantum mechanical methods. The ring strain and the conformational distribution of these cyclic monomers and of the polymers were calculated, and the effect of the medium on the polymerization was predicted, for both bulk and solution. The polymerizability of the three monomers in the gas phase, that is, nonpolar medium, is much greater than that of δ-valerolactone or 1,4-dioxan-2-one. This difference vanishes in the polar medium chloroform, which is attributed to the fact that, while all of these monomers possess polar cis-lactone bonds, the three dilactones possess small dipole moments. The data are combined to give polymerization enthalpy and free energy values. The four stereoregular lactide polymers did not differ significantly in energy. Accordingly, the ability to synthesize any one of these rests on catalyst specificity ("polymer chain-end control"). Although introduction of sterically demanding methyl groups into glycolide is expected to favor coiled conformations and decrease polymerizability, this was not found to be the case. Good agreement of calculated values with experimental data from the literature was achieved.

Keywords Lactides · Polyesters · Quantum mechanics · Ring-opening polymerization · Stereochemistry · Steric effects

Dedicated to Professor Vincenzo Barone and published as part of the special collection of articles celebrating his 60th birthday.

C. Alemán
Departament d'Enginyeria Química, E.T.S. d'Enginyers Industrials de Barcelona, Universitat Politècnica de Catalunya, Diagonal 647, 08028 Barcelona, Spain

C. Alemán (✉)
Center for Research in Nano-Engineering, Universitat Politècnica de Catalunya, Campus Sud, Edifici C', C/Pasqual i Vila s/n, 08028 Barcelona, Spain
e-mail: carlos.aleman@upc.edu

O. Bertran
Departament d'Enginyeria Química, EUETII, Universitat Politècnica de Catalunya, Pça Rei 15, 08700 Igualada, Spain

K. N. Houk
Department of Chemistry and Biochemistry, University of California, Los Angeles, CA 90095-1569, USA

A. B. Padías · H. K. Hall Jr. (✉)
Department of Chemistry and Biochemistry, The University of Arizona, Tucson, AZ 85721, USA
e-mail: hkh@u.arizona.edu

1 Introduction

Polymers are essential materials for modern civilization. Although at present most of the materials in use originate from petroleum, the search for polymers from renewable resources is assuming great urgency. Among these, polylactic acid (PLA) is a shining example of what can be accomplished in this direction [1]. Lactic acid is a renewable resource derived from the starch of either corn or sugar beets, which is fermented to form glucose and consequently converted to lactic acid. Although the polymer can be synthesized by polycondensation from lactic acid, the preferred route is by ring-opening polymerization of its cyclic dimer, lactide, 3,6-dimethyl-1,4-dioxane-2,5-dione. A flowering of research activity has accomplished the lactide polymerization to a variety of stereoisomeric polymers displaying properties ranging from amorphous glasses to highly crystalline materials. These polymers

Scheme 1 Polymerizations and model reactions for glycolide and lactide

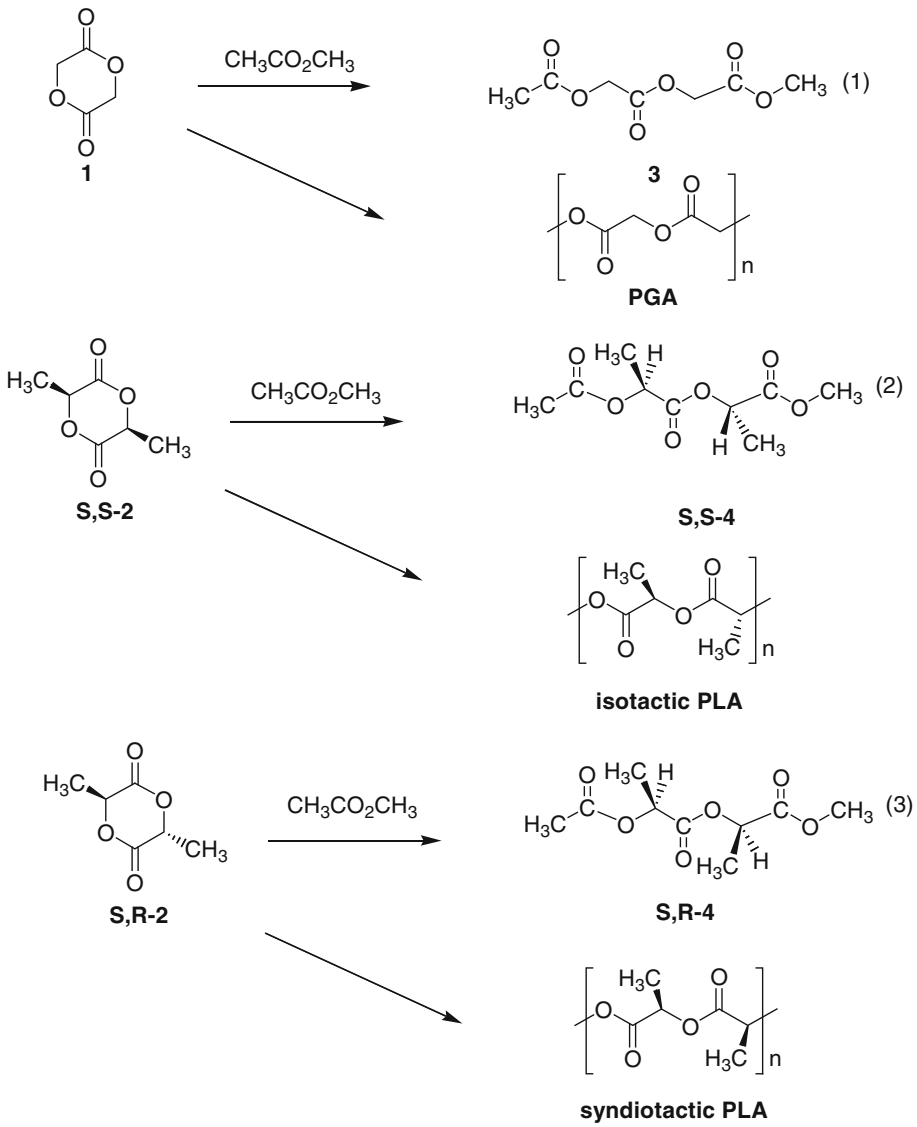

compete as single-use packaging materials, films, and other commodity uses. However, they find their most outstanding use in biomedical devices such as sutures and implants; these devices slowly hydrolyze back to lactic acid and reenter the Krebs cycle. More recently, these polymers have been employed as scaffolds for tissue engineering and in drug delivery systems. Excellent reviews of the many chemical and practical aspects of lactone polymerization have been published [2–13].

The parent lactone lacking substituents, glycolide, or 1,4-dioxane-2,5-dione, **1**, yields only a single polyglycolide (PGA) isomer (Scheme 1). Lactide on the other hand exists as different stereoisomers: the *meso*-lactide, ***S,R-2***, and the two chiral forms, ***S,S-2*** or ***R,R-2***. Polymerization of pure ***S,S-2*** or ***R,R-2*** leads to isotactic PLA in which all the chiral carbons have the same absolute configuration throughout the chain. Syndiotactic PLA, which shows alternate configurations of the sequential stereocenters, is derived from stereoselective polymerization of ***S,R-2***. Finally, heterotactic PLA is obtained by alternating linkages formed by ***R,R*** and ***S,S*** stereocenters. Copolymerization of glycolide with either of the lactides gives further novel materials for biomedical uses.

Recently, we studied the ring-opening polymerization of monolactones by quantum mechanical methods. The ring strain and the conformational distribution of these cyclic monomers and of the polymers were calculated [14–16]. Consistent with extensive studies of carbonyl-containing molecules [17–19], a high preference for *gauche*-coiled conformations was found to strongly influence the outcomes. Finally, the effect of the medium on the polymerization was determined, both in bulk and in solution. These data were combined to give polymerization enthalpy and

free energy changes in good agreement with literature experimental values [14–16].

Our current work applies these methods to the ring-opening polymerization of the dilactones glycolide (**1**) and lactide, the ***S*,*S*-2** and ***S*,*R*-2** stereoisomers being considered for the latter. Beyond calculations analogous to those carried out previously, we calculate the stereochemistry of the propagations leading to the described structures.

2 Methods

Quantum mechanical calculations were performed with Gaussian 03 [20]. All geometry optimizations were performed using the MP2 [21] method combined the 6-31G(d) basis set [22]. Frequency analyses were carried out to verify the nature of all the stationary points and to calculate the zero-point vibrational energies (ZPVE) and both thermal and entropic corrections at 298 K. All thermodynamic corrections were calculated using the standard expressions for an ideal gas in the canonical ensemble. In addition, the electronic energies of all the minima were re-evaluated using single-point calculations at the MP2/6-311++G(d,p) level [23]. Accordingly, the best estimate to the free energy in the gas phase (ΔG^{gp}) was obtained by adding the statistical corrections calculated at the MP2/6-31G(d) level to the latter electronic energies.

To obtain an estimation of the environmental effects, single-point calculations were conducted on the gas-phase optimized structures using a SCRF model. Specifically, the polarizable continuum model (PCM) developed by Tomasi et al. [24–26] was used to simulate chloroform ($\varepsilon = 4.9$) as solvent. The PCM method represents the polarization of the liquid by a charge density appearing on the surface of the cavity created in the solvent. This cavity is built using a molecular shape algorithm. PCM calculations were performed in the framework of the HF/6-311++G(d,p) level using the standard protocol. Within this context, it should be recalled that previous studies indicated that the free energy of solvation (ΔG_{sol}) obtained using solute geometry relaxations in solution and single-point calculations on the optimized geometries in gas phase are almost identical [27–29]. The conformational free energies in chloroform solution (ΔG^{chl}) were estimated using the classical thermodynamics scheme, that is, adding ΔG_{sol} to ΔG^{gp}.

The buildup procedure [30–32] was applied to determine the conformational profile of the model compounds of the polymers. This procedure is based on the assumption that each fragment of a given molecule is conformationally independent of the other fragments in the molecule. Thus, model compounds were divided into fragments. The minimum energy conformations of these small fragments were characterized using a systematic conformational search procedure and joined to form the overall conformations that were taken as starting points for geometry optimizations. In the systematic conformational search procedure, each flexible dihedral angle was expected to have three minima, the number of minima that may be anticipated for the potential energy hypersurfaces (PEHs) of a compound with n flexible dihedral angle being 3^n.

3 Results and discussion

3.1 Conformational analyses of linear monomeric oligomers

The linear diesters **3** and **4** are the repeating units of the PGA and PLA (Scheme 1). However, the calculations were started with the even simpler monomeric units **5** and ***S*-6**, from which the more complex structures can be built up, as shown in Scheme 2.

The minimum energy conformations of **5** and ***S*-6** were determined using a systematic search procedure. Thus, nine starting structures were generated for each compound by combining the three minima of each flexible dihedral angle (χ_1 and χ_2 in Scheme 2), which converged into 5 (one unique and two twofold degenerate) and 7 minima, respectively, after geometry optimization at the MP2/6-31G(d) level. To ascertain the effect of the medium, calculations were carried out for both the gas phase and for chloroform solution.

Table 1 lists the dihedral angles $\{\chi_i\}$, the ΔG^{gp} (gas phase), and the ΔG^{chl} (chloroform solution) of the minimum energy conformations obtained for **5** and ***S*-6**. As can be seen, the two conformations of lower energy are very similar for the two compounds. Thus, the global minimum (**5a** and ***S*-6a**) adopts a partially folded conformation with one dihedral angle χ_1 arranged in *gauche*$^-$ ($\sim -70°$) and the other one extended ($\chi_2 \sim 170°$). In contrast, both χ_1 and χ_2 are folded in the second minimum (**5b** and ***S*-6b**); this conformation is destabilized with respect to the former by <0.7 and 0.5 kcal/mol in the gas phase and chloroform solution, respectively. The fully extended conformations, in which χ_1 and χ_2 show a *trans* conformation, are disfavored with respect to the global minimum by 1.4 (**5c**) and 2.2 kcal/mol (***S*-6f**) in the gas phase. However, the bulk solvent stabilizes these conformers by 0.9 and 0.7 kcal/mol, respectively.

3.2 Conformational analyses of linear dimeric oligomers

Turning to the linear dimers **3** and ***S*,*S*-4**, 25 and 49 starting structures, respectively, were constructed, using the

Scheme 2 Schematics for the calculations

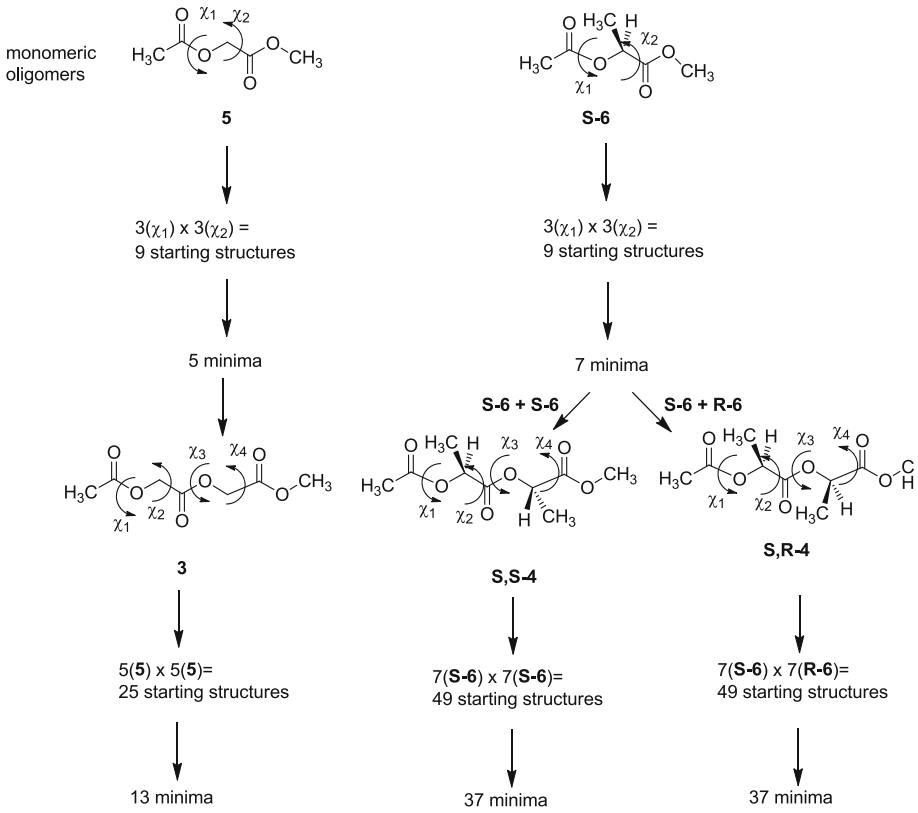

Table 1 Relevant dihedral angles and thermodynamical parameters (in kcal/mol) calculated for the minimum energy conformations of monomeric linear compounds **5** and ***S*-6**

5					***S*-6**				
#	χ_1	χ_2	ΔG^{gp}	ΔG^{chl}	#	χ_1	χ_2	ΔG^{gp}	ΔG^{chl}
5a	−71.4	175.5	0.0[a]	0.0[b]	***S*-6a**	−67.0	166.1	0.0[c]	0.0[d]
5b	−66.6	−17.6	0.7	0.5	***S*-6b**	−63.0	−23.9	0.6	0.2
5c	180.0	−179.9	1.4	0.5	***S*-6c**	52.0	35.2	2.4	1.6
					***S*-6d**	57.0	−158.2	2.8	2.2
					***S*-6e**	−145.7	50.8	1.8	2.0
					***S*-6f**	−151.1	177.8	2.2	1.5
					***S*-6g**	−155.5	−47.4	2.4	2.3

Geometry optimizations and frequency calculations were performed at the MP2/6-31G(d) level. Electronic energies and solvation energies were derived from single-point calculations at the MP2/6-311++G(d,p) and PCM-HF/6-311++G(d,p) levels, respectively

ΔG^{gp} and ΔG^{chl} correspond to the relative free energies in the gas phase and chloroform solution, respectively

[a] $G = -495.014230$ a.u.

[b] $\Delta G_{sol} = -0.31$ kcal/mol

[c] $G = -534.189801$ a.u.

[d] $\Delta G_{sol} = 1.35$ kcal/mol

following buildup procedure: 5(minima of **5**) × 5(minima of **5**) and 7(minima of ***S*-6**) × 7(minima of ***S*-6**). The 49 starting structures of ***S*,*R*-4** were generated using the same process: 7(minima of ***S*-6**) × 7(minima of ***R*-6**), whereby the minima for ***R*-6** are obtained by changing the sign of the dihedral angles of the ***S*-6** minima. Scheme 2 summarizes the procedure used to determine the conformational preferences of these linear model compounds of PGA and PLA.

Application of the buildup procedure led to 13 twofold degenerated minimum energy conformations for **3**. However, only 5 and 8 such minima offer ΔG^{gp} and/or ΔG^{chl} values lower than 1.5 kcal/mol, respectively. Table 2 lists

Table 2 Relevant dihedral angles and thermodynamical parameters (in kcal/mol) calculated for the significant minimum energy conformations of dimeric linear compounds **3**, ***S*,*S*-4** and ***S*,*R*-4**

#	χ_1	χ_2	χ_3	χ_4	ΔG^{gp}	ΔG^{chl}
3						
3a	69.8	−170.8	71.9	−176.8	0.0	0.0
3b	−70.8	174.9	63.6	15.1	1.2	1.3
3c	78.2	170.1	−72.3	175.2	1.4	0.9
3d	−65.1	−21.1	72.4	−175.5	1.4	1.1
3e	70.5	−172.9	63.3	15.9	1.5	1.4
3f	71.0	−174.8	173.3	174.0	2.3	1.1
3g	173.9	167.8	−71.3	177.6	2.3	1.3
3h	66.6	17.6	−71.4	−175.5	2.6	1.5
***S*,*S*-4**						
***S*,*S*-4a**	−65.1	160.4	−67.8	168.8	0.0	0.3
***S*,*S*-4b**	−65.4	161.8	−63.7	−21.6	0.6	0.0
***S*,*S*-4c**	−66.5	−32.7	−64.0	−24.6	1.3	1.0
***S*,*S*-4d**	−65.5	−33.8	−69.9	158.3	1.5	1.0
***S*,*S*-4e**	−60.4	−27.1	54.5	33.9	2.6	1.2
***S*,*S*-4f**	−60.9	−26.0	−144.8	32.4	2.7	1.4
***S*,*R*-4**						
***S*,*R*-4a**	−62.0	−25.6	68.7	−168.0	0.0	0.4
***S*,*R*-4b**	−68.3	170.4	60.5	22.0	0.3	0.8
***S*,*R*-4c**	−61.9	−25.5	65.0	21.7	0.6	0.0
***S*,*R*-4d**	−73.2	−179.7	67.6	−163.2	1.0	0.7
***S*,*R*-4e**	−156.2	−41.3	63.3	22.1	1.5	1.0
***S*,*R*-4f**	−64.2	159.9	−52.5	−33.8	1.6	1.2

Geometry optimizations and frequency calculations were performed at the MP2/6-31G(d) level. Electronic energies and solvation energies were derived from single-point calculations at the MP2/6-311++G(d,p) and PCM-HF/6-311++G(d,p) levels, respectively

the dihedral angles $\{\chi_i$ with $i = 1$–$4\}$, ΔG^{gp} and ΔG^{chl} for these highly populated structures, whose populations add up to 92% when calculated using conformational statistic weights. The lowest energy minimum **3a** in the gas phase (population = 66.5 %) is also the most favored conformation in chloroform solution (population = 47.5%). In this conformation, the two repeating units adopt an identical arrangement with $\{\chi_1, \chi_3\}$ and $\{\chi_2, \chi_4\}$ showing *gauche* and *trans* conformations, respectively. A detailed analysis of the other minima indicates that the population of the coiled conformations, that is, those in which three or more dihedral angles are arranged in *gauche*$^+$ or *gauche*$^-$, is 24% and 26% in the gas phase and chloroform solution, respectively. The population of the extended and semi-extended conformations, in which three or more dihedral angles adopt a *trans* arrangement, increases from 3% (gas phase) to 17% when the bulk solvent is considered. The fully extended conformation is the least favored minimum in the gas phase ($\Delta G^{gp} = 3.7$ kcal/mol), although its stability increases in solution ($\Delta G^{chl} = 1.6$ kcal/mol).

Table 2 includes the minima characterized for ***S*,*S*-4** and ***S*,*R*-4** with ΔG^{gp} and/or ΔG^{chl} lower than 1.5 kcal/mol. Only four and five structures have significant populations in the gas phase (6 in chloroform solution). The buildup procedure for these stereoisomers provided 37 and 39 minima, respectively, distributed in a $\Delta G^{gp}/\Delta G^{chl}$ interval of 7.3/5.7 and 7.1/6.6 kcal/mol, which is significantly larger than the values for **3** (3.7/2.5 kcal/mol). The lowest energy minimum in the gas phase ***S*,*S*-4a** is similar to **3a** and consists of two repeating units with the same conformation, in which $\{\chi_1, \chi_3\}$ and $\{\chi_2, \chi_4\}$ are arranged in *gauche*$^-$ and *trans*, respectively. In contrast, the equivalent conformation ***S*,*R*-4d** is disfavored by 1.0 kcal/mol, while the lowest energy minimum has a different dihedral angle χ_2, which is arranged in *gauche*$^-$. Interestingly, the minimum ***S*,*R*-4a** corresponds to ***S*,*S*-4d**, which is destabilized by 1.5 kcal/mol with respect to ***S*,*S*-4a**. The predicted population for the coiled conformations of ***S*,*S*-4** and ***S*,*R*-4** in the gas phase (chloroform solution) is 36% (66%) and 84% (82%), respectively. Consequently, the population of

Table 3 Selected geometrical parameters around the ester bond for the lowest minimum energy conformations calculated for **1**, ***S*,*S*-2**, and ***S*,*R*-2**

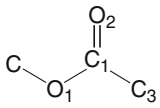

# (in deg.)	**1**[a]	***S*,*S*-2**[a]	***S*,*R*-2**	γ-BL[b]	δ-VL[b]	ε-CL[c]	MA (*s-trans*)	MA (*s-cis*)
O_1–C_1–C_3	114.7	114.7	116.3/116.7	108.9	118.6	118.7	110.5	110.5
O_1–C_1=O_2	121.4	121.0	120.5/121.2	122.4	118.7	122.9	123.4	118.5
O_2=C_1–C_3	123.9	124.3	123.1/122.1	128.7	122.4	118.3	126.0	126.0
C–O_1–C_1–C_3	9.5	7.3	8.1/12.9	2.4	−20.7	−2.8	180.0	0.0
C–O_1–C_1=O_2	−170.2	−172.8	−171.6/−167.1	−177.3	164.8	179.2	0.0	180.0

Parameters for the *s-trans* and *s-cis* conformers of methyl acetate (MA) as well as for γ-butyrolactone (γ-BL), δ-valerolactone (δ-VL) and ε-caprolactone (ε-CL) are also included for comparison

[a] The geometric parameters of the two ester bonds are identical

[b] From reference [14]

[c] From reference [15]

the extended and semi-extended conformations for ***S*,*S*-4** and ***S*,*R*-4** is extremely low, that is, lower than 2% independent of the environment. Thus, the replacement of one hydrogen atom in the repeat unit of PGA by the more sterically demanding methyl group results in drastic changes compared to **3** and enhances the tendency in PLA chains to adopt coiled conformations. Moreover, this tendency seems to be higher in syndiotactic PLA than in isotactic PLA.

3.3 Conformational analysis of cyclic dimers; strain and stability of the dilactones

Table 3 lists the most relevant geometric parameters around the ester group for the minimum energy conformations of **1**, ***S*,*S*-2** and ***S*,*R*-2**, as well as results obtained for optimized s-*cis* and s-*trans* forms of methyl acetate (MA) and other lactones previously reported, *ithat is*, γ-butyrolactone (γ-BL), δ-valerolactone (δ-VL), and ε-caprolactone (ε-CL) [14–16]. The bond and dihedral angles calculated for **1**, ***S*,*S*-2** and ***S*,*R*-2** are different from the values of s-*trans* MA, considered to be the strain-free reference. The strain deformation predicted for these three dilactones is approximately halfway between that found for γ-BL (small ring) and those obtained for δ-VL and ε-CL (larger rings).

Comparison of the free energies calculated for ***S*,*S*-2** and ***S*,*R*-2** indicates that the former is more stable by 1.2 and 2.2 kcal/mol in the gas phase and chloroform solution, respectively. These calculated values are in agreement with crystallographic data, which show that these dilactones consistently adopt a twisted boat form. In the ***S*,*S***-isomer, the two methyl groups adopt cis-diequatorial positions, while the ***S*,*R***-isomer adopts an almost planar twisted boat form with one methyl in equatorial position, while the other one has to be axial [33, 34].

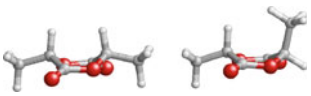

***S*,*S*-2** ***S*,*R*-2**

3.4 Ring-opening reactions

Reactions (1), (2), and (3) of the lactones with methyl acetate (Scheme 1) are simple models for the ring-opening polymerizations of **1**, ***S*,*S*-2**, and ***S*,*R*-2**, respectively. Specifically, reaction (2) models the polymerization of ***S*,*S*-2** to isotactic PLA, while reaction (3) models the polymerization of ***S*,*R*-2** to syndiotactic PLA. The enthalpies and Gibbs free energies in the gas phase (ΔH^{gp}_{rxn} and ΔG^{gp}_{rxn}) and in chloroform solution (ΔH^{chl}_{rxn} and ΔG^{chl}_{rxn}) of the ring-opening reaction for these cyclic compounds were calculated using the minimum energy structures provided by the buildup procedure for **3**, ***S*,*S*-4** and ***S*,*R*-4**. Table 4 lists the ΔH^{gp}_{rxn}, ΔG^{gp}_{rxn}, ΔH^{chl}_{rxn}, and ΔG^{chl}_{rxn} values calculated for reactions (1), (2), and (3).

The ΔG^{gp}_{rxn} values obtained for reactions (1), (2), and (3) are −7.4, −5.1, and −11.2 kcal/mol, respectively, indicating that all three are exergonic processes. These values demonstrate that the polymerizability of the ***S*,*S*-2** dilactone is predicted to be significantly lower than that of its stereoisomer ***S*,*R*-2**, in part because the former is more stable. The intrinsic polymerizability of **1** is predicted to be intermediate between those of the two lactides, while both δ-valerolactone and 1,4-dioxan-2-one display much lower polymerizabilities.

These results show that the incorporation of the methyl substituents does not produce drastic changes from the glycolide dimer **3**, even though the replacement of one

Table 4 Thermochemistry[a] of reactions of methyl acetate with cyclic dimers **1**, ***S*,*S*-2**, and ***S*,*R*-2** (reactions 1, 2, and 3, respectively; Scheme 1) in the gas phase and chloroform solution. Thermochemical parameters for six-membered mono-lactones δ-valerolactone (**δ-VL**, reaction 4)[b] and 1,4-dioxan-2-one (**Dox**, reaction 5)[c] have been included in the table for comparison

		ΔH^{gp}_{rxn}	ΔG^{gp}_{rxn}	ΔH^{chl}_{rxn}	ΔG^{chl}_{rxn}
1	Reaction (1)	−14.6	−7.4	−7.5	−0.5
***S*,*S*-2**	Reaction (2)	−16.1	−5.1	−3.8	−0.8
***S*,*R*-2**	Reaction (3)	−24.0	−11.2	−11.0	0.3
δ-VL	Reaction (4)	−16.2	−1.9	−12.6	−2.7
Dox	Reaction (5)	−13.2	−0.5	−8.5	−0.8

[a] In kcal/mol ΔH^{gp}_{rxn} and ΔG^{gp}_{rxn} are the enthalpy and free energy in the gas phase, respectively. ΔH^{chl}_{rxn} and ΔG^{chl}_{rxn} are the enthalpy and free energy in chloroform solution, respectively

[b] Calculated in reference [14] considering the following reaction as 4:

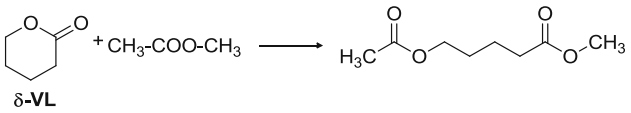

δ-VL

[c] Calculated in reference [15] considering the following reaction as 5:

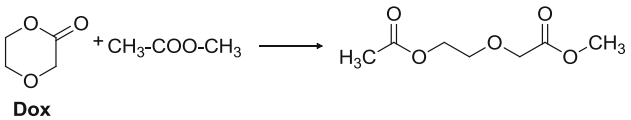

Dox

hydrogen atom in the repeating unit of PGA by the more sterically demanding methyl group enhances the tendency in PLA chains to adopt coiled conformations. This tendency is higher in isotactic PLA, $(–SS–)_n$, than in syndiotactic PLA, $(–SR–)_n$.

The ΔG^{chl}_{rxn} values for reactions (1)–(3) in the more polar medium chloroform are calculated considering statistic weights of the minimum energy conformations found for the linear compounds in chloroform, and they are −0.5, −0.8, and +0.3 kcal/mol, respectively. These values reveal that the solvent plays a very important role in the thermodynamics of the ring-opening reaction of the three dilactones, and the reactions become much less exergonic in a polar solution than in the gas phase. Previously, we have noted the importance of solvation in ring-opening polymerizations: A highly polar lactone (*E*-isomer) is transformed into a linear, much less polar, polymer (*Z*-isomer) [14–16]. Solute–solvent interactions are stronger for the dilactones than for the linear compounds; the ΔG_{sol} values being about 7–9 kcal/mol more favorable for the former than for the latter ones. This is in contrast to our previous studies of δ-valerolactone and 1,4-dioxan-2-one; the ΔG values for these polymerizations are basically the same in the nonpolar gas phase or the polar chloroform solution. The reason for this divergent behavior is that solvation of glycolide and lactide is different from that of monolactones; all of these monomers are highly polar, but glycolide and lactide present stronger interactions with the solvent because of their two ester groups.

The difference between reactions (2) and (3) arises because the interaction with the solvent is more favorable for ***S*,*S*-2** ($\Delta G_{sol} = -6.3$ kcal/mol) than for ***S*,*R*-2** ($\Delta G_{sol} = -5.4$ kcal/mol), possibly because it is more planar and therefore the carbonyl groups are more accessible. The slightly endergonic character calculated for reaction (3) is probably a consequence of the limitations of the SCRF model used in this work; continuum SCRF models not only neglect the configurational sampling of the solvent molecules, but also omit the local anisotropies produced by the solvent molecules of the first solvation shell. The influence of these effects, especially of the latter one, increases with the molecular size and with the number of polar groups [14, 15].

3.5 Stereoisomeric lactide polymers

As described above, reactions (2) and (3) in Scheme 1 are models for the formation of isotactic and syndiotactic PLA, respectively. However, modeling the formation of heterotactic polymer cannot be carried out from the dimers, but requires examination of the appropriate tetramers. The computational difficulties increase rapidly as the number of degrees of freedom in the molecules becomes higher, so we have used an approximation method. Specifically, the buildup procedure was applied considering only the energy minima for ***S*,*S*-4** and ***S*,*R*-4** with $\Delta G^{gp} \leq 1.5$ kcal/mol, that is, ***S*,*S*-4a**–***S*,*S*-4d** and ***S*,*R*-4a**–***S*,*R*-4e**, respectively, in Table 2. Accordingly, a total of $4 \times 4 = 16$ starting

structures were constructed and subsequently optimized at the MP2/6-31G(d) level for the –SSS– and –SRR– tetramers, while $5 \times 5 = 25$ starting structures were considered for the –SRSR– and –SRRS– sequences. The nature of the minimum state of the resulting conformations was not confirmed through frequency analyses, even though single-point calculations were carried out at the PCM-HF/6-311++G(d,p) (chloroform) level. Therefore, this biased search procedure was used to estimate only the ΔH values in both the gas phase and chloroform solution, but not the ΔG values.

The gas phase (empty symbols) and chloroform (filled symbols) energies of the conformations obtained for the four tetramers are shown in Figure 1 relative to the most stable arrangement of the –SRSR– and –SSSS–, respectively. In the gas phase, the most stable conformation of each of the four tetramers is within a relative 1.0 kcal/mol energy interval; this interval increases to 2.7 kcal/mol in

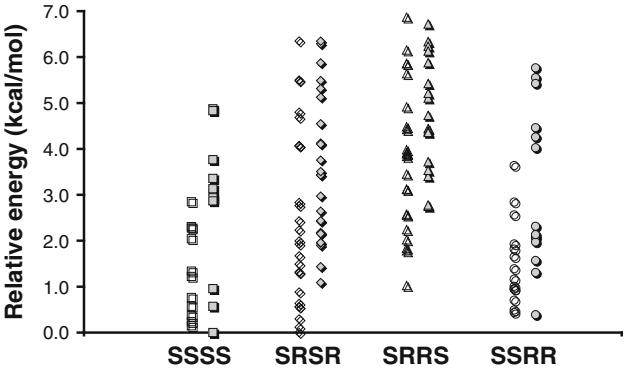

Fig. 1 Relative energies of the conformations optimized at the MP2/6-31G(d) level for the –SSSS–, –SRSR–, –SRRS– and –SSRR– tetramers. Relative energies in the gas phase (*empty symbols*) and chloroform solution (*filled symbols*) are relative to the most stable conformation of the –SRSR– and –SSSS– sequence, respectively. Solvation energies were derived from single-point calculations at the PCM-HF/6-311++G(d,p) level

Table 5 Comparison of the Enthalpies of Reaction (in kcal/mol) for the Dimer and Tetramer Formations in the Gas Phase and in Chloroform

Reaction	ΔH_{rxn}^{gp}	ΔH_{rxn}^{chl}
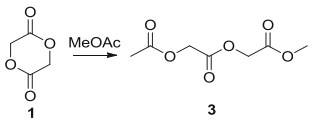	−14.6	−7.5
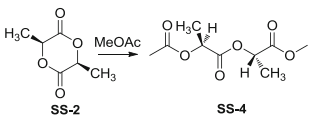	−16.1	−3.8
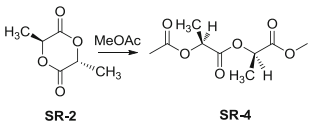	−24.0	−11.0
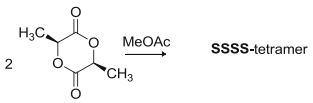	−37.3	−23.7
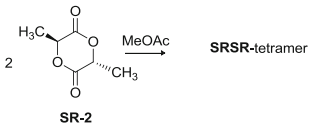	−39.0	−25.0
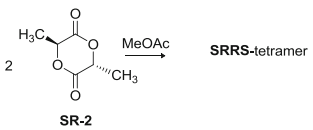	−37.9	−23.5
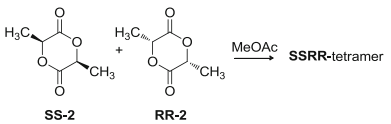	−38.7	−25.6

chloroform solution. Application of conformational statistic weights using Boltzmann probabilities to these sets of conformations indicates that the –SRSR– and –SSSS– tetramers are isoenergetic in the gas phase, while the –SSRR– and –SRRS– are destabilized by only 0.3 and 1.1 kcal/mol. In chloroform solution, the –SSRR–, –SRSR–, and –SRRS– tetramers are destabilized by 0.3, 1.4, and 2.8 kcal/mol, respectively, compared to the –SSSS– one. The similarity among the energies of the more stable structures identified for the different sequences should be attributed to the attractive van der Waals interactions produced by the side methyl groups, which are satisfactorily reproduced at the MP2 level [35–38]. These interactions are maximized by small rearrangements, facilitated by the intrinsic conformational flexibility of the compounds under study.

These small conformational energy differences produced very comparable ΔH^{gp}_{rxn} and ΔH^{chl}_{rxn} values for the four sequences, as reflected in Table 5 for the corresponding formation reactions. Thus, ΔH^{gp}_{rxn} and ΔH^{chl}_{rxn} range from −37.3 to −39.0 and from −23.5 to −25.6 kcal/mol, respectively, that is, the ΔH interval between the different monomer sequences is 1.7 and 2.1 kcal/mol in the gas phase and chloroform, respectively. Comparison of these reaction enthalpies with those obtained for ***S***,***S*****-2** and ***S***,***R*****-2**, also included in Table 5 indicates that the remarkable thermodynamic stereoselectivity found for the dimers is considerably reduced when the polymerization propagates to tetramers, and presumably beyond. This is not unexpected in view of the distance between one chiral center and the next in the growing polymer chain. Accordingly, the ability to prepare the various stereo–isomeric polymers depends on the exquisite tailoring of the sterically crowded chiral polymerization catalysts ("polymer chain-end control").

3.6 Comparison of calculated polymerization enthalpies with experimental values

The calculated polymerization enthalpies for glycolide and lactide (Table 4) can be compared with values from the literature. It should be noted that the calculations were performed in chloroform solution ($\varepsilon = 4.9$) because the dielectric constant of cyclic dilactones decreases very rapidly once the polymerization reaction starts, the final value for PLA being $\varepsilon = 3.1$ [39]. Agreement of these values with one another and with our calculated values is excellent. The experimental value for ΔH_p for polymerization for glycolide in bulk is −6.3 kcal/mol [40], −5.5 kcal/mol for the S,S-lactide [4, 41], and −5.7 kcal/mol for the R,S-lactide [42], with the calculated values being −7.5, −3.8, and −11.0 kcal/mol, respectively.

Lactone polymerization involves converting an *E* ester isomer to the *Z* isomer. The latter is stabilized by 5–8 kcal/mol due to antiparallel dipole alignment, p-orbital on oxygen overlap with the carbonyl group, and lack of steric nonbonded interactions, favoring polymer over monomer. Glycolide and lactides, having two *E* ester groups, might be even more destabilized by ∼10–16 kcal/mole, and the ΔG^{gp}_{rxn} values clearly favor the ring-opening of dilactones with respect to monolactones. However, their antiparallel alignment is a stabilizing factor [2]; so the polymerization enthalpy is less than might be expected for a molecule containing two *E* ester isomers.

Acknowledgments Computer resources were generously provided by the Centre de Supercomputació de Catalunya (CESCA). Financial support from the MICINN and FEDER (MAT2009-09138) and Generalitat de Catalunya (research group 2009 SGR 925 and XRQTC) is gratefully acknowledged. Support for the research of C.A. was received through the prize "ICREA Academia" for excellence in research funded by the Generalitat de Catalunya.

References

1. Duda A, Penczek S (2001) Mechanisms of aliphatic polyester formation. In: Steintuechel A, Doi Y (eds) Biopolymers, vol 3b. Polyesters II—properties and chemical synthesis, Ch 12. Wiley-VCH, Weinheim
2. Dechy-Cabaret O, Martin-Vaca B, Bourissou D (2004) Chem Rev 104:6147–6176
3. Zhong Z, Dijkstra PJ, Feijen J (2004) J Biomat Sci Polym Ed 15:929–946
4. Duda A, Kowalski A, Libiszowski J, Penczek S (2005) Macromol Symp 224:71–84
5. Cirugomane A, Thomas CM, Carpentier J-F (2007) Pure Appl Chem 79:2013–2030
6. Kamber NE, Joong W, Waymouth RM, Pratt RC, Lohmeijer BGG, Hedrick JL (2007) Chem Rev 107:5813–5840
7. Bourrisou D, Moebs-Sanchez S, Martin-Vaca B (2007) Comptes Rendus Chimie 10:775–794
8. Platel RH, Hodgson LM, Williams CK (2008) Polym Rev 48:11–63
9. Chisholm MH, Zhou Z (2008) Stereoselective polymerization of lactide. In: Bough LS, Canich JAM (eds) Stereoselective polymerizations with single-site catalysts. CRC Press, Boca Raton, pp 645–660
10. Stanford MJ, Dove A (2010) Chem Soc Rev 39:486–494
11. Chisholm MH (2010) Pure Appl Chem 82:1647–1662
12. Wheaton C, Hayes P, Ireland B (2009) Dalton Trans 4832–4846
13. Houk KN, Jabbari A, Hall HK Jr, Aleman C (2008) J Org Chem 1573:2674–2678
14. Aleman C, Betran O, Casanovas J, Houk KN, Hall HK Jr (2009) J Org Chem 74:6237–6244
15. Alemán C, Casanovas J, Zanuy D, Hall HK Jr (2005) J Org Chem 70:2950–2956
16. Alemán C, Casanovas J, Hall HK Jr (2005) J Org Chem 70:7731–7736
17. Navarro E, Alemán C, Puiggalí J (1995) J Am Chem Soc 117:7307–7310
18. Alemán C, Navarro E, Puiggali J (1995) J Org Chem 60:6135–6140
19. Alemán C, Navarro E, Puiggalí J (1996) J Phys Chem 100:16131–16136
20. Frisch MJ, Trucks GW, Schlegel HB, Scuseria GE, Robb MA, Cheeseman JR, Montgomery JA, Vreven T Jr, Kudin KN, Burant

JC, Millam JM, Iyengar SS, Tomasi J, Barone V, Mennucci B, Cossi M, Scalmani G, Rega N, Petersson GA, Nakatsuji H, Hada M, Ehara M, Toyota K, Fukuda R, Hasegawa J, Ishida M, Nakajima T, Honda Y, Kitao O, Nakai H, Klene M, Li X, Knox JE, Hratchian HP, Cross JB, Adamo C, Jaramillo J, Gomperts R, Stratmann RE, Yazyev O, Austin AJ, Cammi R, Pomelli C, Ochterski JW, Ayala PY, Morokuma K, Voth GA, Salvador P, Dannenberg JJ, Zakrzewski VG, Dapprich S, Daniels AD, Strain M, Farkas O, Malick DK, Rabuck AD, Raghavachari K, Foresman JB, Ortiz JV, Cui Q, Baboul AG, Clifford S, Cioslowski J, Stefanov BB, Liu G, Liashenko A, Piskorz P, Komaromi I, Martin RL, Fox DJ, Keith T, Al-Laham MA, Peng CY, Nanayakkara A, Challacombe M, Gill PMW, Johnson B, Chen W, Wong MW, Gonzalez C, Pople JA (2003) Gaussian 03, revision B.02. Gaussian Inc., Pittsburgh
21. Møller C, Plesset MS (1934) Phys Rev 46:618–622
22. Hariharan PC, Pople JA (1973) Theor Chim Acta 23:213–222
23. Frisch MJ, Pople JA, Binkley JS (1984) J Chem Phys 80:3265–3269
24. Miertus S, Scrocco E, Tomasi J (1981) Chem Phys 55:117–129
25. Miertus S, Tomasi J (1982) Chem Phys 65:239–245
26. Tomasi J, Mennucci B, Cammi R (2005) Chem Rev 105:2999–3094
27. Hawkins GD, Cramer CJ, Truhlar DG (1998) J Phys Chem B 102:3257–3271
28. Jang YH, Goddard WA III, Noyes KT, Sowers LC, Hwang S, Chung DS (2003) J Phys Chem B 107:344–357
29. Iribarren JI, Casanovas J, Zanuy D, Alemán C (2004) Chem Phys 302:77–83
30. Gibson KD, Scheraga HA (1987) J Comput Chem 8:826–834
31. Vasquez M, Scheraga HA (1988) J Biomol Struct Dyn 5:705–755
32. Vasquez M, Scheraga HA (1988) J Biomol Struct Dyn 5:757–784
33. Chisholm MH, Eilerts NW, Huffman JC, Iyer SS, Pacold M, Phomphrai K (2000) J Am Chem Soc 122:11845–11854
34. Van Hummel GJ, Harkema S (1982) Acta Cryst B38:1679–1681
35. Li AHT, Chao S (2006) J Chem Phys 125:094312
36. Johnson ER, DiLabio GA (2006) Chem Phys Lett 419:333–339
37. Fomine S, Tlenkopatchev M, Martinez S, Fomina L (2002) J Phys Chem A 106:3941–3946
38. Rodríguez-Ropero F, Casanovas J, Alemán C (2008) J Comput Chem 29:69–78
39. Katsuyoshi S, Shigetaka K (2005) IEEE J Trans Fundam Mater 125:204–208
40. Chujo K, Kobayashi H, Suzuki J, Tokuhara S, Tanake M (1967) Makromol Chem 100:262–266
41. Duda A, Penczek S (1990) Macromolecules 23:1636–1639
42. Wang Y, Hillmyer MA (2000) Macromolecules 33:7395–7403